Optimization of the Thermo-Hygromechanical (THM) Process for Sugar Maple Wood Densification

Qilan Fu,[a] Alain Cloutier,[a,*] and Aziz Laghdir [b]

Densified wood is a promising engineered wood product, especially for heavy-duty applications. This study optimized the temperature and duration of the thermo-hygromechanical (THM) densification process applied to sugar maple (*Acer saccharum* Marsh.) wood. The response variables studied were compression set recovery and hardness. The THM densification process was performed at three temperatures (180°C, 200 °C, and 220 °C), densification times (450 s, 900 s, and 1350 s), and post-treatment times (900 s, 1350 s, and 1800 s). Response surface methodology was used to analyze the impact of the three parameters. The effect of temperature on the density profile across thickness was also determined. The results suggested that the optimum densification conditions resulting in high hardness and low compression set recovery were obtained at a temperature of 180 °C, a densification time of 1004 s, and a post-treatment time of 1445 s. Additionally, the density of the densified samples was relatively homogeneous across thickness, although it was dramatically increased compared with control samples. However, density did not increase linearly with temperature. A much higher weight loss occurred at 220 °C, resulting in a significant decrease in density and hardness, whereas little compression set recovery was observed for sugar maple densified at this temperature.

Keywords: Density, Hardness; Compression set recovery; Response surface methodology

*Contact information: a: Centre de Recherche sur les Matériaux Renouvelables (CRMR), Département des Sciences du Bois et de la Forêt, Université Laval, Québec, QC, Canada, G1V 0A6; b: Research scientist, Service de Recherche et d'Expertise en Transformation des Produits Forestiers (Serex), 25 Armand-Sinclair, Porte 5, Amqui, QC, Canada, G5J 1K3; *Corresponding author: alain.cloutier@sbf.ulaval.ca*

INTRODUCTION

Wood densification is a modification technology that compresses wood to obtain a higher density material. It has been used since 1900, when the first patent for the densification process was filed by Sears (Kollman *et al*. 1975). Most of the mechanical properties of wood are proportional to its density (Kollman and Côté 1968; Laine *et al*. 2013; Rautkari *et al*. 2013). The main purpose of densification is to enhance wood density, which improves its mechanical performance and commercial value. Wood species with a high initial density, *e.g*., sugar maple, can also be further improved in terms of hardness, bending strength, and bending modulus of elasticity (MOE) by densification (Fang *et al*. 2011; 2012b).

Many researchers have treated wood with heat and compression to improve its physical and mechanical properties (Navi and Heger 2004; Kamke 2006; Boonstra and Blomberg 2007). This treatment was then called thermo-mechanical densification. Although this method has been found to enhance the mechanical properties of wood, the compressed shape produced by densification is not stable. The wood has been observed to

revert to its original shape when it is remoistened and heated. This phenomenon is known as the shape memory effect (Navi and Heger 2004). Therefore, chemical, physical, or mechanical post-treatments have been needed to prevent wood from recovering its original shape. However, these post-treatments are time-consuming and expensive. Thermo-hygromechanical (THM) compression treatment is a modified method that utilizes steam, heat, and pressure to densify wood. THM compression effectively eliminates the shape memory effect in compressed wood while improving its physical, mechanical, and dimensional stability (Navi and Girardet 2000; Heger *et al*. 2004; Fang *et al.* 2012a; Li *et al*. 2013).

Compression set recovery (CSR) is an important issue in wood densification because it is an indication of wood dimensional stability and determines its potential end-uses. For these reasons, it has been studied rather extensively (Ito *et al.* 1998; Dwianto *et al*. 1998; Higashihara *et al*. 2000; Fang *et al*. 2010; Kutnar and Kamke 2012a; Laine *et al.* 2013; Popescu *et al*. 2014). The release of elastic strain energy stored in amorphous and semi-crystalline cellulose and in microfibrils is the main cause of the set recovery (Laine *et al*. 2013). Three fundamental mechanisms have been proposed to prevent CSR (Norimoto *et al*. 1993): relaxation of internal stresses, formation of cross-linkages between matrix components, and isolation of the wood polymers under the effect of moisture and heat to prevent re-softening. Navi and Heger (2004) reported that hemicellulose hydrolysis occurring during the THM process played an important role in relaxing the internal stresses of the wood components. Hemicelluloses are the least able to withstand heat among the three major components of wood. In the presence of heat and steam, they may degrade severely, and the bonds connecting the molecules of the matrix (hemicelluloses and lignin) may be broken and reformed. In addition, the thermal degradation of the hemicelluloses reduces the hygroscopicity of wood and weakens the connection between the microfibrils and lignin (Navi and Heger 2004), providing additional void space for the rearrangement of microfibrils and the release of internal stresses (Inoue *et al*. 1993).

This study investigated the effects of THM densification temperature and time on the compression set recovery and hardness of densified wood. The impact of temperature and treatment time on the density profile of densified wood was also investigated. This study is part of a larger initiative to optimize the THM densification process for sugar maple wood to obtain high-quality densified wood products.

EXPERIMENTAL

Materials

Thinly sawn strips of sugar maple (*Acer saccharum* March.) wood obtained from a hardwood flooring plant were used. Based on the mass and volume at a relative humidity (RH) of 65% and a temperature (T) of 20 °C, the strips had an average density of 734 kg/m^3 and dimensions of 5.7 mm (radial) × 695.0 mm (longitudinal) × 84.0 mm (tangential). Upon reception, the strips were placed in a climate room at 20 °C and 65% RH until an equilibrium moisture content of approximately 12% was achieved.

Methods

Thermo-hygromechanical densification process

A steam injection press with dimensions 862 mm × 862 mm was used for the densification treatment (Fang *et al*. 2012a). Steam injection holes with a diameter of 1.5

mm were distributed uniformly at 32 mm intervals on both the upper and lower platens of the press. The press platens were preheated to the target temperature before treatment. The densification process was composed of three main steps (Fig. 1): wood softening, wood compression, and post-treatment. Eight strips per test were softened with steam at a maximum pressure of 550 kPa under an increasing mechanical pressure up to 6 MPa. The strips were then compressed to the target thickness (2.85 mm), corresponding to a compression set of 50%. Steam was continuously injected during the whole densification process. After post-treatment, the steam injection was stopped and steam was released through the holes in the platens. Prior to the determination of their properties, all treated specimens were stored in a climate room at 20 °C and 65% RH until their equilibrium moisture content was reached.

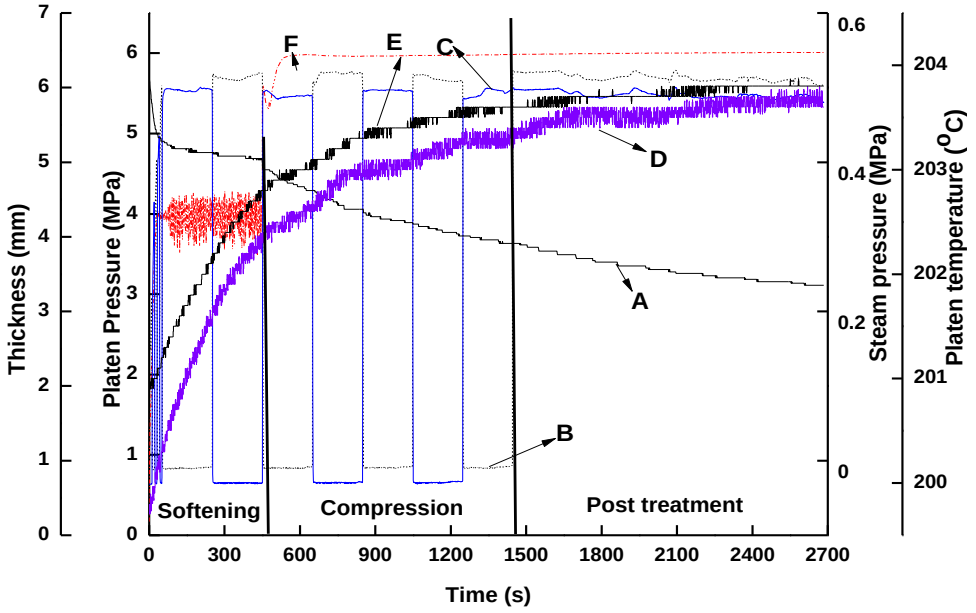

Fig. 1. Thermo-hygromechanical densification process. A: Thickness; B, C: top and bottom platen steam pressure, respectively; D, E: top and bottom platen temperature; F: platen load

Optimization of the THM densification process

The full factorial experimental design is the traditional method used to study main effects and the interactions of several factors on a response variable. However, with an increase in the number of experimental factors, the number of combinations grows rapidly, requiring a considerable amount of experimental time and resources to analyze the data. Response surface methodology (RSM) is a combination of mathematical and statistical techniques that is well suited for situations where a response variable is simultaneously influenced by several factors. Based on the fit of the experimental data to the empirical models, linear or quadratic polynomial equations are used to analyze the response variables. In these equations, the effects of experimental factors and their interactions on the response variables can be statistically evaluated. Consequently, RSM can model and optimize several factor levels to identify the optimum experimental conditions (Del Castillo 2007; Bezerra *et al*. 2008).

In RSM, the Box-Behnken design is most often used for a three-level factorial experiment. This design selects points located on a hypersphere equidistant from center points as experimental arrangements (Bezerra *et al*. 2008). A Box-Behnken experimental design with 3 factors, 3 levels, and 15 runs was chosen to optimize the THM densification process. In this study, the center point was repeated three times to further balance the variance in the middle region of the experiment. Compression set recovery (CSR) and hardness (H) were chosen as response variables because they are of primary importance in applications such as hardwood flooring. The three independent variables and their coded levels are listed in Table 1.

Table 1. Code and Factor Levels Chosen for the Trials

Factor	Code and Level		
	-1	0	+1
A - Temperature (°C)	180	200	220
B - Densification time (s)	450	900	1350
C - Post-treatment time (s)	900	1350	1800

Statistical analysis

The statistical analysis software SAS 9.4 (Cary, NC, USA) was used to perform the normality tests for CSR and the hardness data and to investigate whether a transformation of the response variable was needed and which transformation was suitable using the Box-Cox methodology. Predictions of the response variables in the experimental ranges were also obtained using SAS 9.4. The analysis of the regression and response surface studies were performed using the statistical software Design Expert 8.0.6 (Stat-Ease, Inc, Minneapolis, MN, USA). The response variable was determined by a polynomial equation (Eq. 1),

$$R = \partial_0 + \sum_{i=1}^{3} \partial_i x_i + \sum_{i=1}^{3} \partial_{ii} x_i^2 + \sum_{i,j=1(i\neq j)}^{3} \partial_{ij} x_i x_j \quad (1)$$

where R is the response variable, ∂_0 is a constant, and ∂_i, ∂_{ii}, and ∂_{ij} are the coefficients of linear effect, quadratic effect, and interaction effect, respectively. Finally, x_i and x_j represent the independent variables.

Properties Determination

Brinell hardness test

The hardness of the specimens before and after densification was measured using a test machine (MTS-QTest^{TM}/5, Eden Prairie, MN, USA) with a load cell of 10 kN. The measurements were performed according to EN 1534 (2000), with an indenter of 10 mm in diameter. The maximum load applied was 1000 N, which was reached in 15 s and then maintained for 25 s. Eight replications were performed for each type of specimen, and the average value was used. The Brinell hardness was calculated as follows,

$$H = F/(\pi D h) \quad (2)$$

where H is Brinell hardness (MPa), F is the maximum applied load (N), D is the diameter of the indenter (mm), and h is the maximum depth of the indentation (mm). Once the load was applied to the specimen, the measurement of the depth of the indentation began, and its change over time was recorded by the computer. At the end of the measurement period, the maximum depth of the indentation obtained was used for calculation in Eq. 2.

Compression set recovery

Five swelling/drying cyclic recovery tests were conducted to determine the compression set recovery of wood. After densification, the specimens (50 mm longitudinal × 50 mm tangential) were first dried in an oven to determine their oven-dry thickness before swelling. Oven-dried samples were immersed in water at room temperature for 24 h and oven-dried again for 24 h. The thickness was measured at each wet and oven-dry condition. The compression set recovery was calculated as follows,

$$CSR = [(t_s - t_o) / (t_u - t_o)] \times 100 \quad (3)$$

where CSR is the compression set recovery (%), t_s is the oven-dry thickness after swelling (mm), t_o is the oven-dry thickness before swelling (mm), and t_u is the initial uncompressed thickness (5.7 mm) at T = 20 °C and RH = 65%.

Validation of Model Optimized Parameters

To determine how closely the experimental results fit the model results, the eight specimens were densified according to the optimized parameters obtained from the analysis. The compression set recovery and hardness of the densified samples were measured following the aforementioned methods for validation purposes.

Density Profile

Specimens with dimensions 50 mm × 50 mm were used to measure the density profile before and after densification using an X-ray densitometer (Quintek Measurements Systems model QDP-01x, Knoxville, TN, USA) at intervals of 0.02 mm through the thickness. To investigate the effect of temperature on the density profile, three groups of specimens (eight strips in each group) were densified at temperatures of 180 °C, 200 °C, and 220 °C, respectively. Both densification time and post-treatment time were kept at 900 s for these three groups of specimens.

RESULTS AND DISCUSSION

Response Results

The average compression set recovery and hardness values obtained for each treatment are presented in Table 2. The CSR of densified sugar maple ranged from 1.1% for the No. 13 test (densification temperature: 220 °C; densification time: 900 s; post treatment time: 1800 s) to 19.2% for the No. 10 test (200 °C, 1350 s, and 900 s, respectively). The maximum value of CSR was approximately 17 times that of the minimum CSR. The hardness of the densified samples varied from 25.2 MPa for the No. 13 test to 51.4 MPa for the No. 12 (densification temperature: 180 °C, densification time: 1350 s, and post treatment time: 1350 s). The maximum value of hardness was approximately twice the minimum value. The values of CSR and hardness varied as a function of the process parameters used. Furthermore, lower CSR values and higher hardness values were not obtained under the same experimental conditions. Therefore, it was necessary to analyze the effects of the process parameters on CSR and hardness and further optimize the densification process to achieve the best balance between the two response variables. At first glance, a relatively high hardness and low compression set recovery was obtained simultaneously for treatment Nos. 11, 12, 14, and 15.

Table 2. Average Compression Set Recovery and Hardness Obtained for the Treatments Applied

No.	Temperature (°C)	Densification time (s)	Post-treatment time (s)	Compression set recovery (%) (n=5)	Hardness (MPa) (n=8)
1	200	450	900	13.0 (4.5)	35.7 (7.1)
2	200	1350	1800	14.4 (4.5)	33.5 (5.0)
3	220	900	900	3.7 (1.2)	33.3 (10.1)
4	220	1350	1350	2.3 (1.5)	31.2 (12.3)
5	180	900	900	10.6 (1.3)	39.3 (6.1)
6	200	450	1800	10.4 (2.9)	50.4 (4.6)
7	200	900	1350	12.3 (4.4)	46.9 (5.9)
8	180	450	1350	15.5 (3.1)	49.4 (3.2)
9	220	450	1350	4.6 (2.9)	36.3 (14.1)
10	200	1350	900	19.2 (3.0)	39.0 (5.7)
11	180	900	1800	8.6 (2.0)	46.2 (3.2)
12	180	1350	1350	5.7 (4.5)	51.4 (4.7)
13	220	900	1800	1.1 (0.7)	25.2 (6.3)
14	200	900	1350	7.9 (3.4)	46.8 (5.0)
15	200	900	1350	8.9 (2.3)	46.9 (6)

*Standard deviations given in parentheses

Analysis of variance and quadratic model for compression set recovery

Normality tests performed on CSR data showed that a natural logarithm transformation was needed for the CSR data. An analysis of variance was performed for the impact of temperature, densification time, and post-treatment time on the natural logarithm of CSR (lnCSR). Table 3 shows the main effects of the three factors on lnCSR and their interaction effects. The significant terms were A ($p = 0.0101$) and A^2 ($p = 0.0164$), indicating that temperature had a significant linear and quadratic effects on lnCSR at a confidence level of 95%. Neither of the other two factors and none of the interactions between two of the three factors were statistically significant. The coefficient of determination (R^2) of the model was 0.88, which indicated that 88% of the lnCSR variation was explained by the model.

A second-order polynomial regression equation was determined to express lnCSR as a function of temperature (A), densification time (B), and post-treatment time (C) at their coded levels (value range between -1 and 1):

$$\text{lnCSR} = +2.25 - 0.65\,A - 0.12\,B - 0.24\,C + 0.077\,AB - 0.25\,AC - 0.016\,BC - 0.85\,A^2 + 0.3\,B^2 + 0.074\,C^2 \qquad (R^2 = 0.88) \qquad (4)$$

In Eq. 4, the terms with a negative coefficient resulted in a decrease in lnCSR. The coefficients with a larger absolute value had more of an impact on the lnCSR. Combined with the results of Table 3, it was concluded that temperature was the dominant parameter controlling lnCSR and CSR.

Table 3. Analysis of Variance Results of lnCSR *versus* Temperature (*A*), Densification Time (*B*), and Post-treatment Time (*C*)

Source	Sum of squares	DF	Mean square	F value	*p* value	Remarks
A	3.42	1	3.42	16.20	0.0101	Significant
B	0.12	1	0.12	0.57	0.4856	
C	0.47	1	0.47	2.21	0.1971	
A x *B*	0.024	1	0.024	0.11	0.7517	
A x *C*	0.25	1	0.25	1.19	0.3245	
B x *C*	0.001	1	0.001	0.005	0.9467	
A^2	2.66	1	2.66	12.59	0.0164	Significant
B^2	0.34	1	0.34	1.62	0.2589	
C^2	0.02	1	0.02	0.095	0.7709	

Effect of process factors on compression set recovery and reliability of the quadratic model

According to the analysis of variance results presented in Table 3, the interaction effects between temperature, densification time, and post-treatment time on lnCSR were not significant. Therefore, the three-dimensional response surface plots of lnCSR against two of the three parameters considered are not presented. Figure 2a presents the effects of temperature, densification time, and post-treatment time on lnCSR (a), recalling that densification time and post-treatment time had no significant effect on lnCSR. As shown in Fig. 2a, lnCSR decreased dramatically when the densification temperature exceeded 200 °C (factor coded level = 0). The lowest lnCSR was obtained for the specimens densified at 220 °C for a post-treatment time of 1800 s, suggesting a permanent compression set. The lower lnCSR obtained at a high temperature (220 °C) might have been due to the hydrolysis of hemicellulose. As a result, the hygroscopicity of the wood decreased, and the connection between the microfibrils and lignin weakened, providing additional void space for the rearrangement of the microfibrils and release of the internal stresses (Navi and Heger 2004). Therefore, the shape memory effect was reduced, and the dimensional stability improved. According to Inoue *et al.* (1993), the decreased hygroscopicity of the wood could be attributed to the transformation of highly hygroscopic hemicellulose into low-hygroscopic furfural substances after the high temperature treatment. This was in agreement with the current results, which showed that only the linear and quadratic effects of temperature had a significant impact on lnCSR.

Figure 2b shows the predicted values calculated from Eq. 4 against the actual values of lnCSR. Most of the points are arranged along a straight line, representing a perfect prediction, which indicated that the quadratic model (Eq. 4) was appropriate for predicting the variation of lnCSR. However, some actual values deviated from the predicted values, which caused a decrease of the R^2 of the model to 0.88.

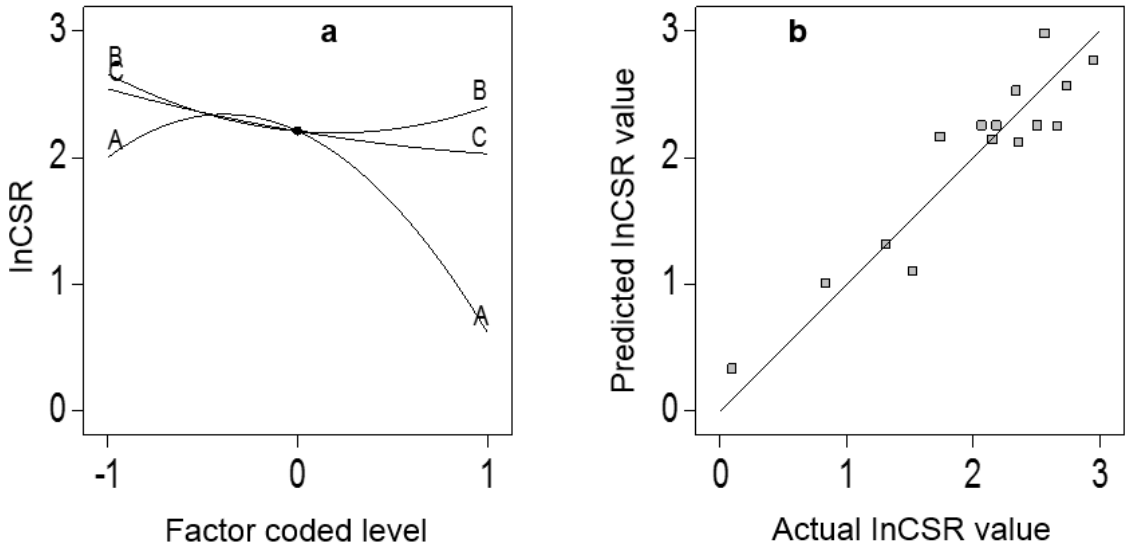

Fig. 2. (a) Effect of temperature (*A*), densification time (*B*), and post-treatment time (*C*) on lnCSR; (b) Comparison between actual and predicted values of lnCSR

Table 4. Analysis of Variance for Results of Hardness *versus* Temperature (*A*), Densification Time (*B*), and Post Treatment Time (*C*)

Source	Sum of squares	DF	Mean square	F value	*p* value	Remarks
A	454.51	1	454.51	70.43	0.0004	Significant
B	34.86	1	34.86	5.40	0.0677	
C	8.00	1	8.00	1.24	0.3162	
A x *B*	12.60	1	12.60	1.95	0.2211	
A x *C*	56.25	1	56.25	8.72	0.0318	Significant
B x *C*	102.01	1	102.01	15.81	0.0106	Significant
A^2	65.78	1	65.78	10.19	0.0242	Significant
B^2	1.20	1	1.20	0.19	0.6839	
C^2	163.08	1	163.08	25.27	0.0040	Significant

Analysis of variance and quadratic model for hardness

The normality tests performed on hardness data showed that no transformation was needed for the hardness in order to meet the assumption of a normal distribution. An analysis of variance was performed on the impact of temperature, densification time, and post-treatment time on the hardness (Table 4). The *p* value of A was 0.0004, which indicated that temperature had a very significant impact on hardness at a confidence level of 95%. Given the results presented in Table 2, the hardness decreased significantly when

the temperature exceeded 200 °C. The results in Table 4 also showed that the interaction terms of temperature (*A*) × post treatment time (*C*) (P = 0.0318) and densification time (*B*) × post treatment time (*C*) (*p* = 0.0106) were significant. The R^2 of the model was 0.96, which indicated that only 4% of the total hardness variation could not be explained by the model.

A second-order polynomial equation was determined to express the hardness as a function of temperature (*A*), densification time (*B*), and post-treatment time (*C*) at their coded levels (value range between -1 and 1):

$$\text{Hardness} = +46.87 - 7.54\ A - 2.09\ B + 1.00\ C - 1.77\ A\ B - 3.75\ A\ C - 5.05\ B\ C - 4.22\ A^2 - 0.57\ B^2 - 6.65\ C^2 \quad (R^2=0.96) \quad (5)$$

In Eq. 5, the terms with a negative coefficient are those that resulted in a decrease in hardness. The coefficients with a larger absolute value had more of an impact on hardness.

Effect of process factors on hardness and reliability of the quadratic model

According to the analysis of variance results presented in Table 4, the interaction between temperature and densification time was not significant. Therefore, the three-dimensional response surface plots of hardness against these two parameters are not presented.

Figure 3 presents the interaction effects of (a) temperature and post-treatment time on hardness; (b) densification time and post-treatment time on hardness; (c) temperature, densification time, and post treatment time on hardness; and (d) the comparison between actual and predicted values of hardness. In general, the mechanical properties of wood tended to increase as density increased. Previous works (Fang *et al*. 2012b; Kutnar and Kamke 2012a; Rautkari *et al.* 2013) have shown that the surface density of wood increases after densification treatment. Therefore, the hardness of densified wood was expected to increase following THM densification. Fukuta *et al.* (2007) reported that hardness did not increase linearly with density. The extent of the change in wood hardness was dependent upon many factors, including species and densification process parameters (Kamke 2006). For instance, softwood species exhibit a higher increase in hardness following densification.

As shown in Figs. 3a and 3c, hardness decreased with increasing temperature. This result is in agreement with the results reported by Fang *et al.* (2012a) and Li *et al.* (2013). The reason for the decrease in hardness as temperature increased could be explained by the advanced degradation of lignin and hemicelluloses (Fang *et al.* 2012b). Additionally, acetic acid is released during the degradation of hemicellulose. This can impact the cellulose microfibrils in the amorphous regions by breaking the bonds joining the units of glucose, resulting in shorter cellulose chains and therefore in a lower degree of polymerization of cellulose. As shown in Figs. 3b and 3c, the variation in densification time had little impact on hardness. Also, a higher hardness value could be obtained at a middle level of post-treatment time. In Fig. 3d, the actual hardness values were quite close to the predicted values, which indicated that the quadratic model developed for hardness had a higher reliability than the model developed for lnCSR. The R^2 of the regression model (Eq. 5) was 0.96, which demonstrated that it was appropriate.

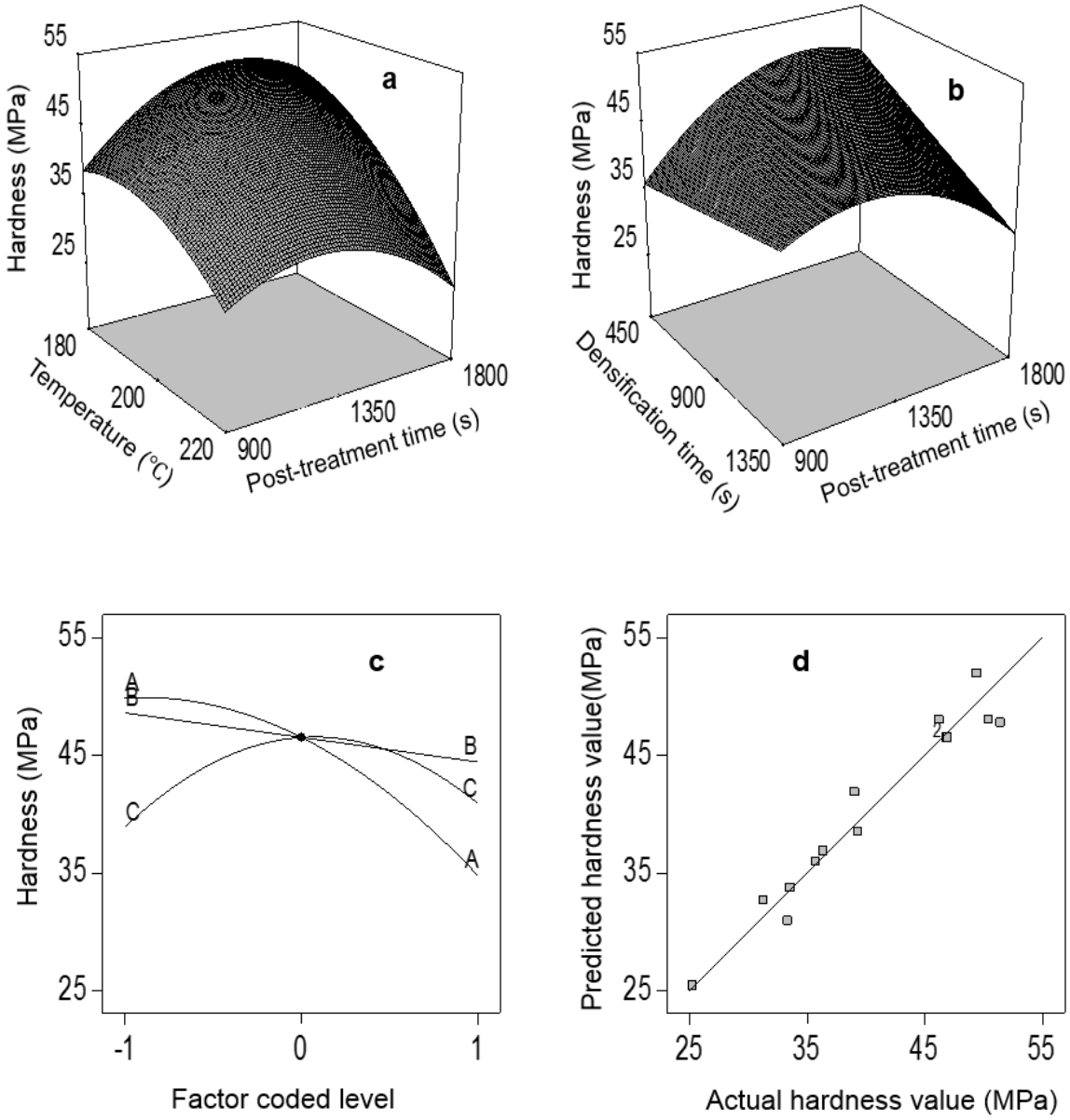

Fig. 3. a) Response surface plots of hardness versus temperature and post-treatment time; b) response surface plots of hardness versus densification time and post-treatment time; c) effect of temperature (*A*), densification time (*B*), and post-treatment time (*C*) on hardness; and d) comparison between actual and predicted values of hardness

Desirability functions of compression set recovery and hardness

To find optimal conditions on multi-response variables, general transformations of the response variables into desirability functions can be performed (Derringer 1980). In this study, based on the experimental data, predictions of response variables obtained from the regression equations (Eqs. 4 and 5) in the experimental ranges considered for temperature, densification time, and post-treatment time are presented in Table 5. The 5^{th} and 95^{th} percentiles of the predicted values of the response variables were used to develop the desirability functions described below.

Table 5. Predictions of Response Variables in the Experimental Ranges

Response variable	Minimum	5th pctl	10th pctl	25th pctl	50th pctl	75th pctl	90th pctl	95th pctl	Maximum
lnCSR	0.36	1.05	1.31	1.84	2.26	2.44	2.59	2.68	3.05
Hardness (MPa)	16.26	33.30	35.46	39.22	43.65	47.47	49.74	50.82	53.58

pctl: percentile

Hardness should be maximized, while CSR should be minimized. Thus, the desirability functions were constructed as follows (Derringer 1980; Bezerra *et al.* 2008),

$$d_1 = \begin{cases} 0 & \text{if } \widehat{H_p} < 33.30 \\ \left(\frac{\widehat{H_p} - 33.30}{50.82 - 33.30}\right) & \text{if } 33.30 < \widehat{H_p} < 50.82 \\ 1 & \text{if } \widehat{H_p} > 50.82 \end{cases} \quad (6)$$

where $\widehat{Hp}$ is the predicted hardness (Eq. 5), d_1 is the desirability coefficient for hardness, and

$$d_2 = \begin{cases} 1 & \text{if } \widehat{\ln CSR} < 1.05 \\ \left(\frac{\widehat{\ln CSR} - 2.68}{1.05 - 2.68}\right) & \text{if } 1.05 < \widehat{\ln CSR} < 2.68 \\ 0 & \text{if } \widehat{\ln CSR} > 2.68 \end{cases} \quad (7)$$

where $\widehat{\ln CSR}$ is the predicted lnCSR (Eq. 4) and d_2 is the desirability coefficient for lnCSR. The overall desirability for response variables D is defined as a function of d_1 and d_2 as follows,

$$D = (d_1^{w_1} d_2^{w_2})^{\frac{1}{2}} \quad (8)$$

where D is the overall desirability for the response variables, w_1 is the weight coefficient for hardness, and w_2 is the weight coefficient for lnCSR. The weight coefficients show the degree of importance given to the response variable by the user.

CSR and hardness are considered equally important in applications such as hardwood flooring. In this case, their weight coefficients can be considered equal to one ($w_1 = w_2 = 1$). Thus, Eq. 8 can be expressed as:

$$D = (d_1 d_2)^{\frac{1}{2}} \quad (9)$$

The optimum solutions (a high hardness while maintaining a relatively low lnCSR value) were obtained from SAS 9.4 using the Grid-search method, which could be used to find an optimum for the overall desirability (Park and Park 1998). Based on the predicted data for hardness and lnCSR and Eqs. 6, 7, and 9, the corresponding values of d_1, d_2, and D could be calculated. Using the desirability functions approach, the optimum conditions of temperature, densification time, and post-treatment time were determined as: 180 °C, 1004 s, and 1445 s, respectively. Under these conditions, lnCSR and hardness were predicted to be 2.03 and 50.55 MPa, respectively (Eqs. 4 and 5).

Table 6 presents the results of the predicted values of the response variables and the overall desirability obtained from all the experimental design conditions (Table 2, Nos. 1-13) as well as those from the optimum conditions (No. 14). Because both high hardness and low compression set recovery were desired in this study, the values of d_1 and d_2 were expected to be close to one, or the highest possible value of D was desired. The values of d_1 and d_2 did not reach one value simultaneously under any given experimental conditions. The lowest lnCSR value was obtained at the highest temperature (220 °C), when the hardness value was too small. Finally, the overall desirability D reached its highest value (0.63) under the optimum conditions.

Validation of the approach was performed by the THM densification of eight specimens under the optimum conditions mentioned above. The experimental result for lnCSR under the optimum conditions was 2.95 (s = 0.22), which was higher than the predicted value (2.03). This deviation might have been due to the relatively lower accuracy of the quadratic model for lnCSR (R^2 = 0.88). The experimental hardness obtained was 52.12 (s = 15.12) MPa, which was close to the predicted value (50.55 MPa).

Table 6. Results of Predicted Values of Response Variables and the Overall Desirability Obtained from the Experimental Design Conditions and Optimum Conditions for w_1=w_2=1

No.	Temperature (°C)	Densification time (s)	Post-treatment Time (s)	Predicted hardness (MPa)	Predicted lnCSR	d_1	d_2	D
1	200	450	900	35.69	2.97	0.14	0	0
2	200	1350	1800	33.51	2.25	0.01	0.26	0.06
3	220	900	900	31.21	1.31	0	0.84	0
4	220	1350	1350	30.68	1	0	1	0
5	180	900	900	38.79	2.11	0.31	0.35	0.33
6	200	450	1800	47.79	2.52	0.83	0.10	0.28
7	200	900	1350	46.87	2.25	0.77	0.26	0.45
8	180	450	1350	49.94	2.55	0.95	0.08	0.28
9	220	450	1350	38.40	1.09	0.29	0.98	0.53
10	200	1350	900	41.61	2.76	0.47	0	0
11	180	900	1800	48.29	2.13	0.86	0.34	0.54
12	180	1350	1350	49.3	2.15	0.91	0.33	0.54
13	220	900	1800	25.71	0.33	0	1	0
14	180	1004	1445	50.55	2.03	0.98	0.4	0.63

Density Profiles

There is a common agreement that the density of wood has a major impact on its mechanical and physical properties. To characterize density across thickness and investigate the effect of treatment temperature on density, the density profiles of the control samples and samples densified at different temperatures (180 °C, 200 °C, 220 °C) were measured (Fig. 4). The density of the control sample was almost constant throughout the thickness, with the exception of the lower density values in the vicinity of both surfaces. The density of THM-densified samples increased compared to the control sample and was fairly constant across thickness but decreased sharply near the surface. Furthermore,

different treatment temperatures resulted in different density profiles. These differences could be observed by comparing the surface and core densities. The lower densities observed on both surfaces of the densified wood could have been due to the degradation of polymers at the wood surfaces in contact with the hot platens and to the thickness recovery close to the surface, as proposed by Kutnar and Kamke (2012b). The wood density did not increase linearly with treatment temperature. The highest core density and the highest surface density gradient were obtained at 200 °C rather than at 220 °C. A higher percentage of weight loss occurred at 220 °C, which might have been induced by the degradation of wood components, resulting in a decrease in the overall density.

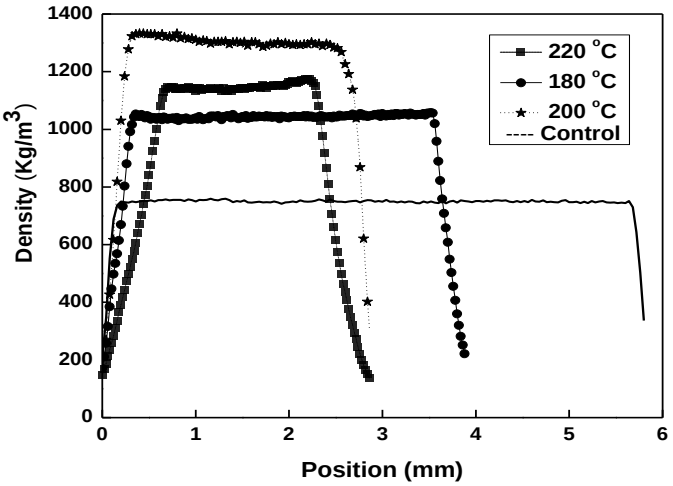

Fig. 4. Typical density profile through the thickness of the control sample and samples densified at 180, 200, and 220 °C

CONCLUSIONS

1. The optimum densification conditions were: temperature at 180 °C, densification time of 1004 s, and a post treatment time of 1445 s. The predicted results of lnCSR and hardness based on the optimum conditions were 2.03 and 50.55 MPa, respectively. The highest value of overall desirability (0.63) obtained corresponded to the optimum conditions.
2. The high hardness value and low compression set recovery were difficult to obtain simultaneously under the given experimental conditions. The lower lnCSR value could be obtained at a higher temperature (220 °C), but the hardness decreased dramatically.
3. The accuracy of the quadratic model for hardness was better than that for the compression set recovery, which indicated that hardness could be predicted more easily and accurately.
4. Temperature was the dominant parameter influencing compression set recovery and hardness of the densified wood.

5. The density of the densified samples was dramatically increased compared to the control sample and was fairly constant across the thickness but decreased sharply near the surface. A higher percentage of weight loss occurred at 220 °C, resulting in an important decrease in the density and hardness of wood. However, almost no compression set recovery was observed for the sugar maple densified at 220 °C.

ACKNOWLEDGEMENTS

The authors thank Mr. Gaétan Daigle from the Service de Consultation Statistique, Département de Mathématiques et Statistique, Université Laval for guidance in the statistical analysis of the data. They also thank Mr. David Lagueux for technical assistance with the densification process. The authors are grateful to the Natural Sciences and Research Council of Canada (NSERC) for funding this research under Discovery Grant #121954-2012.

REFERENCES CITED

Bezerra, M. A., Santelli, R. E., Oliveira, E. P., Villar, L. S., and Escaleira, L. A. (2008). "Response surface methodology (RSM) as a tool for optimization in analytical chemistry," *Talanta* 76(5), 965-977. DOI: 10.1016/j.talanta.2008.05.019

Boonstra, M. J., and Blomberg, J. (2007). "Semi-isostatic densification of heat-treated radiata pine," *Wood Science and Technology* 41(7), 607-617. DOI: 10.1007/s00226-007-0140-y

Del Castillo, E. (2007). "An overview of empirical process optimization," in: *Process Optimization: A Statistical Approach* (Vol. 105), Springer Science and Business Media, Springer, New York. DOI: 10.1007/978-0-387-71435-6

Derringer, G. (1980). "Simultaneous optimization of several response variables," *Journal of Quality Technology* 12(4), 214-219.

Dwianto, W., Morooka, T., and Norimoto, M. (1998). "The compressive stress relaxation of albizia (*Paraserianthes falcata* Becker) wood during heat treatment," *Journal of the Japan Wood Research Society* 44(6), 403-409.

EN 1534 (2000). "Wood and parquet flooring. Determination of resistance to indentation (Brinell)," CEN-European Committee for Standardization, Brussels.

Fang, C. H., Mariotti, N., Cloutier, A., Koubaa, A., and Blanchet, P. (2010). "Densification of wood veneers combined with oil-heat treatment. Part 1: Dimensional stability," *BioResources* 6(1), 373-385. DOI: 10.15376/biores.6.1.373-385

Fang, C. H., Cloutier, A., Blanchet, P., and Barbuta, C. (2011). "Densified engineered wood flooring for heavy-duty use," (http://valuetowood.ca/html/english/research_development/search_projects_details.php?prj_id=157), Accessed on May 20, 2016.

Fang, C. H., Mariotti, N., Cloutier, A., Koubaa, A., and Blanchet, P. (2012a). "Densification of wood veneers by compression combined with heat and steam," *European Journal of Wood and Wood Products* 70(1-3), 155-163. DOI: 10.1007/s00107-011-0524-4

Fang, C. H., Blanchet, P., Cloutier, A., and Barbuta, C. (2012b). "Engineered wood flooring with a densified surface layer for heavy duty use," *BioResources* 7(4), 5843-5854. DOI: 10.15376/biores.7.4.5843-5854

Fukuta, S., Takasu, Y., Sasaki, Y., and Hirashima, Y. (2007). "Compressive deformation process of Japanese cedar (*Cryptomeria japonica*)," *Wood and Fiber Science: Journal of the Society of Wood Science and Technology* 39(4), 548-555.

Heger, F., Groux, M., Girardet, F., Welzbacher, C., Rapp, A. O., and Navi, P. (2004). "Mechanical and durability performance of THM-densified wood," in: *Final Workshop Cost Action E22: Environmental Optimization of Wood Protection*, Lisboa, Portugal.

Higashihara, T., Morooka, T., and Norimoto, M. (2000). "Permanent fixation of transversely compressed wood by steaming and its mechanism," *Wood Research*: *Bulletin of the Wood Research Institute Kyoto University* 87, 28-29.

Inoue, M., Norimoto, M., Tanahashi, M., and Rowell, R. M. (1993). "Steam or heat fixation of compressed wood," *Wood and Fiber Science: Journal of the Society of Wood Science and Technology* 25(3), 224-235.

Ito, Y., Tanahashi, M., Shigematsu, M., and Shinoda, Y. (1998). "Compressive-molding of wood by high-pressure steam-treatment: Part 2. Mechanism of permanent fixation," *Holzforschung* 52(2), 217-221. DOI: 10.1515/hfsg.1998.52.2.217

Kamke, F. A. (2006). "Densified radiata pine for structural composites," *Maderas. Ciencia y Tecnologia* 8(2), 83-92. DOI: 10.4067/S0718-221X2006000200002

Kollman, F. F. P., Kuenzi, E. W., and Stamm, A. J. (1975). "Veneer, plywood and laminates," in: V. Springer (ed.), *Principles of Wood Science and Technology, Vol. 2: Wood Based Materials*, Heidelberg, Germany. DOI: 10.1007/978-3-642-87931-9

Kollmann, F. F. P., and Côté, W. A. (1968). "Physics of wood," in: V. Springer (ed.), *Principles of Wood Science and Technology, Vol. 1: Solid Wood*, Heidelberg, Germany. DOI: 10.1007/978-3-642-87928-9

Kutnar, A., and Kamke, F. A. (2012a). "Influence of temperature and steam environment on set recovery of compressive deformation of wood," *Wood Science and Technology* 46(5), 953-964. DOI: 10.1007/s00226-011-0456-5

Kutnar, A., and Kamke, F. A. (2012b). "Compression of wood under saturated steam, superheated steam, and transient conditions at 150 °C, 160 °C and 170 °C," *Wood Science and Technology* 46(1-3), 73-88. DOI: 10.1007/s00226-010-0380-0

Laine, K., Belt, T., Rautkari, L., Ramsay, J., Hill, C. A., and Hughes, M. (2013). "Measuring the thickness swelling and set-recovery of densified and thermally modified Scots pine solid wood," *Journal of Materials Science* 48(24), 8530-8538. DOI: 10.1007/s10853-013-7671-4

Li, L., Gong, M., Yuan, N., and Li, D. (2013). "An optimal thermo-hydro-mechanical densification (THM) process for densifying balsam fir wood," *BioResources* 8(3), 3967-3981. DOI: 10.15376/biores.8.3.3967-3981

Navi, P., and Heger, F. (2004). "Combined densification and thermo-hydromechanical processing of wood," *MRS Bulletin* 29(5), 332-336. DOI: 10.1557/mrs2004.100

Navi, P., and Girardet, F. (2000). "Effects of thermo-hydro-mechanical treatment on the structure and properties of wood," *Holzforschung* 54(3), 287-293. DOI: 10.1515/HF.2000.048

Norimoto, M., Ota, C., Akitsu, H., and Yamada, T. (1993). "Permanent fixation of bending deformation in wood by heat treatment," *Wood Research*: *Bulletin of the Wood Research Institute of Kyoto University* 79, 23-33.

Park, S. H., and Park, J. O. (1998). "Simultaneous optimization of multiple responses using a weighted desirability function," in: *Quality Improvement through Statistical Methods*, Birkhäuser, Boston, pp. 299-311. DOI: 10.1007/978-1-4612-1776-3_24

Popescu, M. C., Lisa, G., Froidevaux, J., Navi, P., and Popescu, C. M. (2014). "Evaluation of the thermal stability and set recovery of thermo-hydro-mechanically treated lime (*Tilia cordata*) wood," *Wood Science and Technology* 48(1), 85-97. DOI: 10.1007/s00226-013-0588-x

Rautkari, L., Laine, K., Kutnar, A., Medved, S., and Hughes, M. (2013). "Hardness and density profile of surface densified and thermally modified Scots pine in relation to degree of densification," *Journal of Materials Science* 48(6), 2370-2375. DOI: 10.1007/s10853-012-7019-5

Article submitted: May 31, 2016; Peer review completed: July 19, 2016; Revised version received and accepted: August 3, 2016; Published: August 31, 2016.
DOI: 10.15376/biores.11.4.8844-8859